

See discussions, stats, and author profiles for this publication at: <https://www.researchgate.net/publication/231660112>

Marcus Inverted Region in the Photoinduced Electron Transfer Reactions of Ruthenium(II) – Polypyridine Complexes with Phenolate Ions

ARTICLE *in* THE JOURNAL OF PHYSICAL CHEMISTRY A · OCTOBER 1997

Impact Factor: 2.69 · DOI: 10.1021/jp971746v

CITATIONS

41

READS

45

7 AUTHORS, INCLUDING:



Pounraj Thanasekaran

Academia Sinica

47 PUBLICATIONS 926 CITATIONS

SEE PROFILE



Thangamuthu Rajendran

PSNACET

39 PUBLICATIONS 643 CITATIONS

SEE PROFILE



Chockalingam Srinivasan

Madurai Kamaraj University

105 PUBLICATIONS 1,083 CITATIONS

SEE PROFILE



Perumal Ramamurthy

University of Madras

110 PUBLICATIONS 1,849 CITATIONS

SEE PROFILE

Marcus Inverted Region in the Photoinduced Electron Transfer Reactions of Ruthenium(II)–Polypyridine Complexes with Phenolate Ions

P. Thanasekaran,[†] T. Rajendran,[†] S. Rajagopal,^{*,†} C. Srinivasan,[‡] R. Ramaraj,[†] P. Ramamurthy,[§] and B. Venkatachalapathy[§]

School of Chemistry and Department of Materials Science, Madurai Kamaraj University, Madurai 625 021, India, and Department of Inorganic Chemistry, University of Madras, Madras 600 025, India

Received: May 30, 1997[®]

Ruthenium(II)–polypyridyl complexes of similar size but with variable reduction potential undergo efficient photoinduced electron-transfer reactions with phenolate ions in aqueous medium. All these reactions are exergonic and are in accordance with the Marcus theory of electron transfer. At high negative ΔG° Marcus inverted region is observed in this bimolecular photoinduced charge separation reaction.

Introduction

Photoinduced electron transfer (ET) is one of the very active areas of research in chemistry in this decade.^{1–4} The rate of electron transfer from a donor molecule to an acceptor in a solvent is controlled by several factors and the most important of them are the free energy change of the reaction (ΔG°), the reorganization energy (λ), and the ET distance (d) between the donor and acceptor. The electron-transfer rate constant (k_{et}) in both the classical and semiclassical theories can be represented by eq 1

$$k_{\text{et}} = K_{\text{el}} \nu_n \exp[-\Delta G^\ddagger/(RT)] \quad (1)$$

where k_{el} is the electronic transmission coefficient, ν_n the nuclear frequency, and ΔG° the free energy of activation. When the electron-transfer distance, d , is kept constant, the rate of an electron-transfer process is decided by ΔG° and λ through the Marcus equation (eq 2)^{5–7}

$$\Delta G^\ddagger = (\lambda + \Delta G^\circ)^2/(4\lambda) \quad (2)$$

Substitution of this expression into eq 1 provides the basic relation (eq 3) for treating k_{et} in terms of ΔG° and λ :

$$k_{\text{et}} = K_{\text{el}} \nu_n \exp[-(\lambda + \Delta G^\circ)^2/(4\lambda RT)] \quad (3)$$

The value of $K_{\text{el}} \nu_n$ is usually taken as $1.0 \times 10^{11} \text{ s}^{-1}$.

Marcus theory predicts that k_{et} will follow a bell-shaped energy dependence as a function of ΔG° , initially increasing as ΔG° becomes more negative in the normal region and decreasing with increasing driving force in the inverted region.⁸ According to Marcus theory, the maximum of the bell-shaped curve occurs when λ equals $-\Delta G^\circ$ where the free energy of activation (ΔG^\ddagger is zero. When $-\Delta G^\circ > \lambda$, the Marcus inverted region may be observed. The experimentalists have realized that only for photoinduced ET reactions or for radiochemically generated energetic systems would a reaction have large enough exoergicity to display this parabolic behavior.^{8–13} Although evidence for the inverted region is substantial in charge-shift reactions and charge-recombination reactions, it is almost nonexistent for bimolecular charge separation reactions except

in the recent report by Turro et al. in the photoinduced redox reactions of Ru(II) complexes with cytochrome *c* in its oxidized and reduced forms.¹⁴ The following four reasons have been attributed for the difficulty of observing the inverted region for charge separation reactions at high exoergicity:¹⁵ (i) diffusion is the rate-limiting step, (ii) lack of a truly homogeneous series in particular chemical donors or acceptors, (iii) λ is an increasing function of the separation distance (d) between the reactants, and (iv) extra reaction channels become accessible at higher $-\Delta G^\circ$ values. If these problems are circumvented by choosing the appropriate reactants, it is possible to observe the Marcus inverted region in the bimolecular reactions.¹⁴

According to classical Marcus theory ET can occur only at the intersection point of the two potential energy surfaces. There may be a more effective route via quantum mechanical nuclear tunneling from the reactant surface to the product surface, in which case eq. 4 may apply:³

$$k_{\text{et}} = (2\pi/\hbar) |H_{\text{rp}}|^2 (4\pi\lambda_0 kT)^{-1/2} \sum_{m=0}^{m=\infty} (e^{-s} s^m / m!) \exp[-(\lambda_0 + \Delta G^\circ + m\hbar\nu)^2 / (4\lambda_0 kT)] \quad (4)$$

where H_{rp} is the electronic coupling energy, m is an integer, and $s = \lambda/\hbar\nu$. This condition is likely to be particularly important in the inverted region, where the vibrational wave functions of the reactant and product states are embedded, so the Franck–Condon factors are much larger than in the normal region. In the normal region ($-\Delta G^\circ < \lambda$) eq 4 is represented by the simplified expression, eq 5:

$$k_{\text{et}} = (2\pi/\hbar) |H_{\text{rp}}|^2 (4\pi\lambda_0 kT)^{-1/2} \exp[-(\lambda_0 + \Delta G^\circ)^2 / (4\lambda_0 kT)] \quad (5)$$

It has been well established that the excited-state properties of ruthenium(II) complexes such as lifetime and redox potentials can be tuned by judicious choice of ligands.^{16,17} Ruthenium(II)–polypyridyl complexes in the excited state have extensively been used as efficient electron donors and acceptors with appropriate inorganic and organic substrates as artificial systems for the conversion and storage of solar energy and to test the Marcus theory of ET.^{1–4,16–20} Though phenols are not efficient quenchers for $^*\text{Ru}(\text{bpy})_3^{2+}$ (bpy = 2,2'-bipyridine), several phenolate ions undergo efficient electron-transfer reactions and Marcus theory has successfully been applied to this photoredox

[†] School of Chemistry, Madurai Kamaraj University.

[‡] Department of Materials Science, Madurai Kamaraj University.

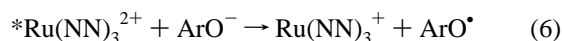
[§] Department of Inorganic Chemistry, University of Madras.

[®] Abstract published in *Advance ACS Abstracts*, September 15, 1997.

system.^{21–23} Tris(2,2'-bipyrazine)ruthenium(II) ion, $\text{Ru}(\text{bpz})_3^{2+}$, in the excited state, is a more powerful oxidant ($E^\circ = 1.40$ V) compared to the well-known complex $\text{Ru}(\text{bpy})_3^{2+}$ ($E^\circ = 0.80$ V). When we measured the rate constant, k_q , for the reductive quenching of $^*\text{Ru}(\text{bpz})_3^{2+}$ with PhO^- , we were surprised to note that the k_q value for the reduction of this complex is smaller than that for $\text{Ru}(\text{bpy})_3^{2+}$ though the former is more exoergic by 0.6 V. Hence, to check whether we realize the Marcus inverted region in this particular redox system, we have studied the photosensitized electron-transfer reactions of six $\text{Ru}(\text{NN})_3^{2+}$ (NN = polypyridyl ligand) with several phenolate ions by choosing Ru(II) complexes of similar size but substantially variable reduction potentials from 0.69 to 1.40 V.²⁴ Indeed we have observed the Marcus inverted region in this bimolecular photoinduced ET reactions, and the important findings are reported in this article.

Experimental Details

Materials. The tris-chelated Ru(II) complexes of 2,2'-bipyridine, 4,4'-dimethyl-2,2'-bipyridine, 1,10-phenanthroline, 2,2'-bipyrazine, 2,2'-bipyrimidine, and 2,3-bis[2-pyridyl]pyrazine were synthesized as their chloride salt and purified by column chromatography.²⁵ Phenols were purified by vacuum distillation or by recrystallization before use. The phenolate ions were prepared by mixing stoichiometric amounts of phenols and NaOH. The pH of the reaction mixture was maintained at 12.5. The absorption and emission spectral measurements were performed using JASCO Model 7800 UV-vis spectrophotometer and JASCO FP-770 spectrofluorometer, respectively. The solutions used for lifetime and emission measurements were deaerated by bubbling dry N_2 gas for 20 min. The change of emission intensity of $^*\text{Ru}(\text{bpz})_3^{2+}$ with the change of [quencher] measured at 298 K is shown in Figure 1. The quenching rate constant, k_q , for the reaction (eq 6)



was determined by the luminescence-quenching technique from the Stern–Volmer eq 7 using emission intensity and lifetime data.

$$\tau^\circ/\tau \text{ or } I^\circ/I = 1 + k_q\tau^\circ[\text{ArO}^-] \quad (7)$$

where I° and I are the emission intensities in the absence and presence of the quencher and τ° and τ are the emission lifetimes of Ru(II) complexes in the absence and presence of the quencher.

As expected for a bimolecular reaction, the Stern–Volmer plots for the luminescence quenching of $^*\text{Ru}(\text{NN})_3^{2+}$ with various phenolate ions are linear, and the sample plots shown in Figure 2.

Laser Flash Photolysis Studies. Excited-state lifetimes of Ru(II) complexes were determined by observing the time dependence of the luminescence decay using a Czerny–Turner monochromator with a stepper motor control and a Hamamatsu R-928 photomultiplier tube. The 355 nm radiation (8 ns pulses) from an Applied Photophysics SP-Quanta Ray GCR-2(10) Nd:YAG laser was used as the excitation source. A DHS 2 dichroic harmonic separator was used to separate the third harmonic from the second harmonic and the fundamental of the Nd:YAG laser. The 355 nm output was directed toward the sample using prisms. The signals were captured using a Hewlett-Packard 54201A 100 MHz digital storage oscilloscope. The oscilloscope is optically triggered using the photodiode. The data were transferred to the computer and analyzed using the software described elsewhere.²⁶

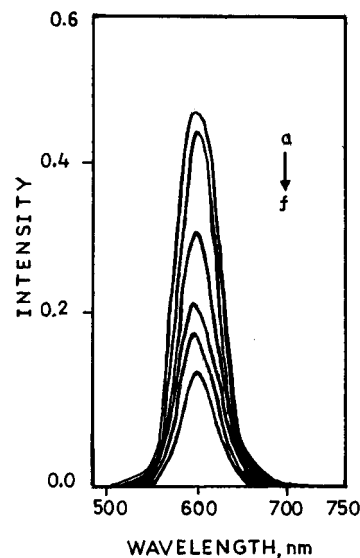


Figure 1. Change of emission intensity of $^*\text{Ru}(\text{bpz})_3^{2+}$ in the presence of 2,6-dimethylphenolate ion at different concentrations: (a) 0, (b) 4×10^{-4} , (c) 8×10^{-4} , (d) 12×10^{-4} , (e) 16×10^{-4} , and (f) 20×10^{-4} M.

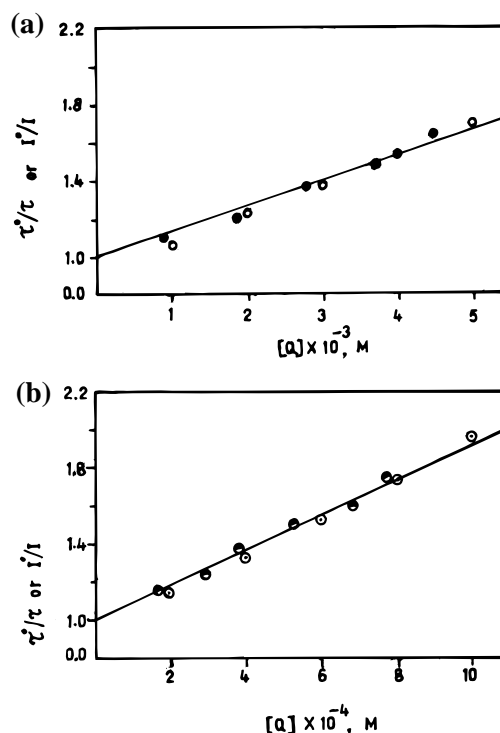


Figure 2. (a) Stern–Volmer plot for the reductive quenching of $\text{Ru}(\text{bpz})_3^{2+}$ with phenolate ion in aqueous solution: (○) luminescence quenching; (●) lifetime quenching. (b) Stern–Volmer plot for the reductive quenching of $\text{Ru}(\text{bpz})_3^{2+}$ with *p*-methoxyphenolate ion in aqueous solution: (○) luminescence quenching; (●) lifetime quenching.

The production of the excited state on exposure to 355 nm was measured by monitoring (pulsed xenon lamp of 250 W) the absorbance change of the nitrogen-bubbled sample solution. The change in the absorbance of the sample on laser irradiation was used to calculate the rate constant as well as the time-resolved absorption transient spectrum. The change in the absorbance on flash photolysis was calculated using the expression

$$\Delta A_t = \log[I/I_0 - 1]$$

where ΔA_t is the change in the absorbance at time t . I_0 is the

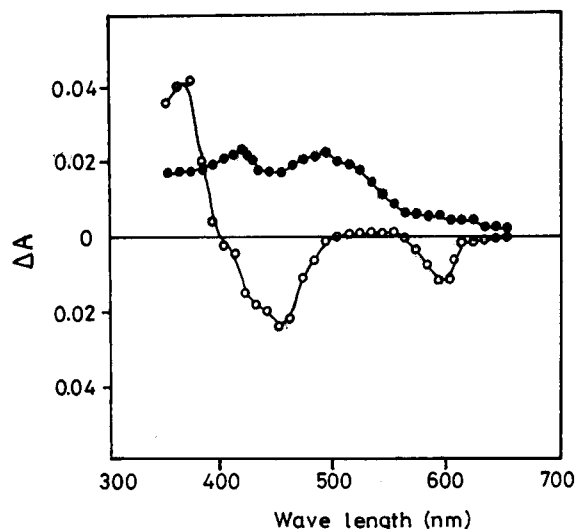


Figure 3. Transient absorption spectrum obtained 2 μ s after 355 nm laser flash photolysis of Ar-purged solutions containing 20 mM Ru-(bpz) $_3^{2+}$ and 0.002 M *p*-OMeC $_6$ H $_4$ O $^-$ at pH = 12.5.

voltage before flash, and I is the difference in voltage at time t after the flash.

A plot of $\ln(\Delta A_t - \Delta A_\infty)$ vs time gives a straight line. The slope of the straight line gave the rate constant for the decay. The reciprocal of these values gave the lifetime of the triplet. The time-resolved transient absorption spectrum was recorded by plotting the change in absorbance at a particular time vs wavelength (Figure 3).

Electrochemical Measurements. The oxidation potentials of phenolate ions were determined by a cyclic voltammetric technique using an EG & G Princeton Applied Research potentiostat/galvanostat Model 273A and Model RE 0151 recorder. The stock solutions of the phenolates for the electrochemical studies were prepared in water, and the pH of the solution was maintained at 12.5 by adding the appropriate quantity of NaOH solution. Potassium chloride was used as the supporting electrolyte. A glassy carbon electrode and a standard calomel reference electrode were used in the electrochemical measurements. Cyclic voltammograms were recorded after purging the solution with dry nitrogen gas for 20 min. The cyclic voltammograms of these phenolate ions are irreversible, and the observed oxidation potentials are corrected to account for the dimerization of the phenoxyl radicals (vide infra).

Results and Discussion

The structure of ligands of Ru(NN) $_3^{2+}$ complexes used in the present study are shown in Figure 4. The absorption and emission spectral data and the excited-state lifetimes and redox potentials of six Ru(II) complexes are collected in Table 1. The bimolecular quenching rate constants, k_q , for the reductive quenching of six *Ru(NN) $_3^{2+}$ by four phenolate ions measured from the linear Stern–Volmer plots obtained from emission-quenching and from lifetime measurements in aqueous medium are given in Table 2. The electron-transfer nature of the reaction is established by recording the absorption spectrum of the transient using the time-resolved laser flash photolysis technique, and in Figure 3 a representative transient spectrum for the system of Ru(bpz) $_3^{2+}$ and *p*-methoxyphenolate ion is shown. The spectrum of the transient is similar to the reported absorption spectra of Ru(bpz) $_3^+$ and *p*-OMePhO $^\bullet$; the $\lambda_{\text{max}}^{\text{ab}}$ value for Ru-(bpz) $_3^+$ and *p*-OMePhO $^\bullet$ are 490 and 415 nm, respectively. Similar transient spectra have been observed with other Ru-(NN) $_3^{2+}$ and phenolate systems, and the maxima correspond to Ru(NN) $_3^+$ and phenolate ions. These data are similar to already

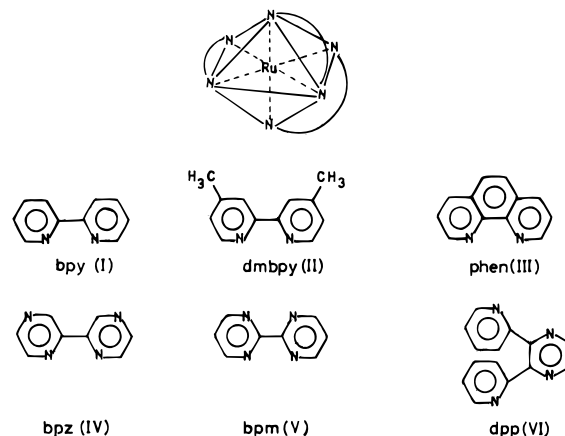


Figure 4. Structure of ligands used in the present study.

TABLE 1: Absorption and Emission Spectral Data, Lifetimes, and Redox Properties of Ru(II) Complexes in Aqueous Solution at 298 K

Ru(II) complex	λ_{ab} , nm	λ_{em} , nm	τ , μ s	$E^{\circ 2+/+}$, ^a V
Ru(bpy) $_3^{2+}$	451	600	0.68	0.80
Ru(dmbpy) $_3^{2+}$	458	611	0.33	0.69
Ru(phen) $_3^{2+}$	443	587	1.18	0.79
Ru(bpz) $_3^{2+}$	452	599	0.94	1.40
Ru(bpm) $_3^{2+}$	450	603	0.06	1.20
Ru(dpp) $_3^{2+}$	456	619	0.27	1.13

^a E° values are taken from ref 25.

reported results.^{21,27,28} Since it is established that the quenching occurs by ET, the redox-quenching reaction can be discussed as shown in Scheme 1.

Since the reactants are oppositely charged species (Ru(NN) $_3^{2+}$ and ArO $^-$), we wanted to check the formation of the ground-state complex between them. There is no appreciable change in the absorption spectra of Ru(NN) $_3^{2+}$ due to the addition of ArO $^-$ used in the present study. Furthermore, the Stern–Volmer plots (from lifetime and emission intensity data) (Figure 2) are linear for all photoredox systems studied here, indicating that under the present experimental conditions dynamic quenching is the predominant process excluding the contribution of static quenching to the overall luminescence-quenching reaction.

In Scheme 1, k_{12} is the diffusion rate constant, k_{21} is the rate constant for dissociation of the precursor complex, and k_{23} and k_{32} are the rate constants for the forward and back electron-transfer process. The observed reaction rate constant is given in terms of diffusional and electron-transfer rate constants

$$k_{\text{obs}} = k_{12}/(1 + k_{12}/k_{23}K_{\text{eq}}) \quad (8)$$

$K_{\text{eq}} = k_{12}/k_{21}$ is the equilibrium constant for the formation of the precursor complex. Substitution of the expression for electron transfer (eq 3) in eq 8 leads to the expression for the observed rate constant

$$k_{\text{obs}} = k_q = \frac{k_{12}}{1 + [k_{12}/(K_{\text{eq}}K_{\text{el}}\nu_n)]\exp[(\lambda + \Delta G^\circ)^2/(4\lambda RT)]} \quad (9)$$

Since the reaction is between two oppositely charged ions, the value of diffusion rate constant (k_{12}) may be calculated by the Debye equation (eq 10)^{7,28}

$$k_{12} = [2RT/(3000\eta)][2 + r_Q/r_R + r_R/r_Q] \quad (10)$$

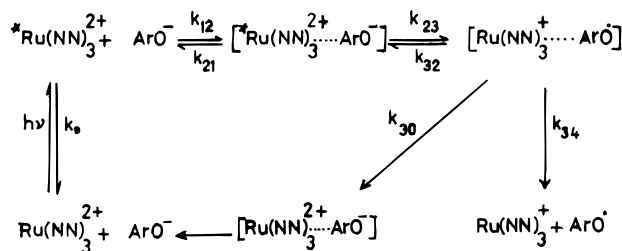
where η is the viscosity of the solvent and r_Q and r_R are the radius of the quencher and sensitizer, respectively. By use of

TABLE 2: k_q and ΔG° (eV) Values for the Reductive Quenching of $^*\text{Ru}(\text{NN})_3^{2+}$ Complexes by Phenolate Ions in Aqueous Solution at 298 K (pH = 12.5)

quencher ^a	$k_q \times (10^{-8} \text{ M}^{-1} \text{ s}^{-1})$											
	$\text{Ru}(\text{bpy})_3^{2+}$		$\text{Ru}(\text{dmbpy})_3^{2+}$		$\text{Ru}(\text{phen})_3^{2+}$		$\text{Ru}(\text{bpz})_3^{2+}$		$\text{Ru}(\text{bpm})_3^{2+}$		$\text{Ru}(\text{dpp})_3^{2+}$	
	$-\Delta G^\circ$ (eV)	k_q	$-\Delta G^\circ$ (eV)	k_q	$-\Delta G^\circ$ (eV)	k_q	$-\Delta G^\circ$ (eV)	k_q	$-\Delta G^\circ$ (eV)	k_q	$-\Delta G^\circ$ (eV)	k_q
phenolate (0.35 V)	0.45	2.5	0.34	1.8	0.44	7.8	1.05	1.6	0.85	57.0	0.75	33.0
4-methylphenolate (0.27 V)	0.53	12.0	0.42	2.3	0.52	16.0	1.13	6.4	0.93	72.0	0.83	37.0
4-methoxyphenolate (0.14 V)	0.66	21.0	0.55	8.8	0.65	26.0	1.26	6.7	1.06	88.0	0.96	39.0
2,6-dimethylphenolate (0.25 V)	0.55	27.0	0.44	14.0	0.54	24.0	1.15	8.2	0.95	44.0	0.85	30.0

^a Values in parentheses are the oxidation potentials of phenolate ions in aqueous solution. The reversible oxidation potentials reported by Arnett et al.³² are 0.405, 0.330, 0.110, and 0.240 V, respectively.

SCHEME 1: ET Mechanism of Luminescence Quenching



the value of the viscosity (η) of water as $1.0 \times 10^{-3} \text{ N s m}^{-2}$ and the radii of $\text{Ru}(\text{NN})_3^{2+}$ and ArO^- as 0.71 and 0.38 nm, respectively, the value of k_{12} comes to $9.0 \times 10^9 \text{ M}^{-1} \text{ s}^{-1}$.

The value of ΔG° can be calculated from the redox potentials of reactants and the work terms (eq 11)

$$\Delta G^\circ = E^\circ_{\text{ArO}^-/\text{ArO}^-} - E^\circ_{\text{Ru}(\text{NN})_3^{2+}/\text{Ru}(\text{NN})_3^+} + W_p - W_r \quad (11)$$

where W_p and W_r are the work terms required to bring the products (Ru^+ , Q^+) and reactants (Ru^{2+} , Q) together at the separation distance. Since the reaction has been carried out in aqueous medium, the contribution from work terms to ΔG° is negligible. The values of ΔG° calculated from eq 11 are collected in Table 2. The term λ is the sum of inner sphere (λ_i) and outer sphere (λ_o) reorganization energies, and λ_o is given by eq 12:

$$\lambda_o = (\Delta e)^2 [(1/2)r_R + (1/2)r_Q - 1/d] (1/D_{op} - 1/D_s) \quad (12)$$

where Δe , D_{op} , and D_s are the number of electrons transferred, the optical dielectric constant (1.77 for H_2O), and the static dielectric constant (78.5 for H_2O), respectively. The value of λ_o calculated from eq 12 for these redox systems is 0.87 eV. Though λ_i is negligible in the case of $\text{Ru}(\text{NN})_3^{2+}$, it is significant with ArO^- and calculated to be 0.2 eV.²⁹ Jakobsen et al. recently calculated the intramolecular reorganization energy for ET reactions involving organic systems, and the value for phenol systems was $\sim 0.2 \text{ eV}$.³⁰ The C–O bond length in the phenoxyl radical is 1.23 Å, while the value in the phenolate anion is 1.36 Å.³¹ The oxidation potentials of ArO^- measured in the present study deserve comment. Comparison of our irreversible oxidation potentials for ArO^- with the reversible potentials obtained by Arnett et al.³² shows that though there is a difference of 60 mV in the case of PhO^- and $p\text{-MeC}_6\text{H}_4\text{O}^-$, the difference is negligible with $p\text{-OMeC}_6\text{H}_4\text{O}^-$ and $2,6\text{-(Me)}_2\text{C}_6\text{H}_3\text{O}^-$. Recently, Bordwell and Cheng³³ have realized the sizable radical-stabilizing effects for OMe and ortho-substituted alkyl groups. In the case of some phenolate ions the deviation between the reversible potentials and irreversible potentials observed here (60 mV) is due to the competitive dimerization of phenoxyl radicals. It is well-known that phenoxyl radicals undergo fast dimerization reaction to form the corresponding dimers.^{32,34} The

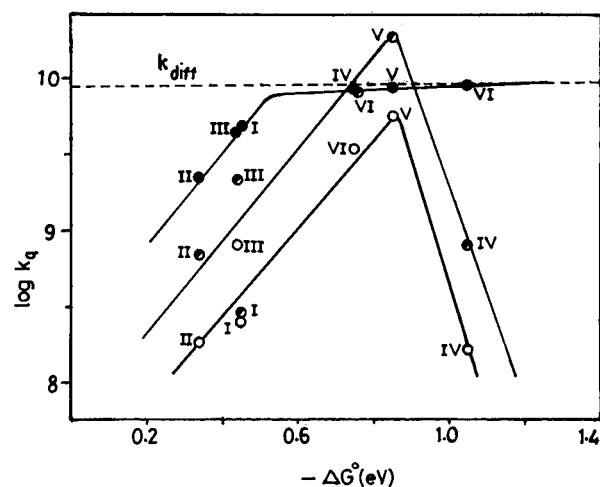


Figure 5. Plot of $\log k_q$ vs $-\Delta G^\circ$. k_q values are calculated using steady-state equation (●), quantum mechanical equation (◐), and experimental methods (○).

shift of the observed cathodic peak potential E_{pc} with respect to the standard potential E_c° caused by dimerization with the rate constant k_{dim} and the bulk concentration C_0 is given by eq 13:

$$E_{pc} - E_c^\circ = \frac{RT}{3\eta F} \left[\ln \frac{k_{dim} C_0 RT}{\nu n F} - 3.12 \right] \quad (13)$$

where n is the number of electrons, ν the scan rate, and F the Faraday constant. The values of the rate constant for the dimerization of a variety of phenoxyl radicals are known, and from these values the deviation in the oxidation potential can be calculated. These values fall in the range 50–150 mV. Thus, the oxidation potential values of ArO^- measured in the present study are close to the reversible oxidation potentials in aqueous medium. The reduction potentials of $^*\text{Ru}(\text{NN})_3^{2+}$ and oxidation potentials of ArO^- in aqueous solution measured in the present study and collected from literature are given in Tables 1 and 2.

By application of eqs 9–12, the rate constants for ET from ArO^- to $^*\text{Ru}(\text{NN})_3^{2+}$ have been estimated and plotted against $-\Delta G^\circ$ (Figure 5) for all six $\text{Ru}(\text{II})$ complexes by taking phenolate and p -methoxyphenolate as the electron donors. The k_q values calculated from eq 4 have also been plotted against $-\Delta G^\circ$ in Figure 5. The plots of experimental and calculated rate constants versus $-\Delta G^\circ$ are bell-shaped for all phenolate ions. Thus, the Marcus inverted region is observed when $-\Delta G^\circ > \lambda$. On the other hand, if $-\Delta G^\circ < \lambda$, the points fall in the normal region. Comparison of the λ values of these redox systems with the ΔG° values collected in Table 2 points out that the condition $-\Delta G^\circ > \lambda$ is satisfied only with the $^*\text{Ru}(\text{bpz})_3^{2+}$ – ArO^- system. Thus, the low k_q value observed at high negative ΔG° value in the $^*\text{Ru}(\text{bpz})_3^{2+}$ – ArO^- photoredox system can be taken as one more experimental observation for the Marcus inverted region in the case of intermolecular charge

separation reaction next to the recent report by Turro and co-workers.¹⁴ The data presented in the Figure 5 indicate that the observed rate constant is maximum at $\Delta G^\circ = -0.87$ eV with PhO^- but at -1.05 eV with $p\text{-OMePhO}^-$. These values correspond to the λ values of the respective redox system and close to the theoretically calculated values (vide infra). The interesting aspect is that the λ value increases from 0.85 to 1.05 eV if the OMe group is introduced in the quencher. A similar increase in λ value with the change of size and structure of the organic quencher has also been realized by Gould et al. and other workers.^{35–37}

In the present system we have selected the Ru(II) complexes in such a way that though the excited-state reduction potential varies from 0.69 to 1.40 V, all six Ru(II) complexes have similar radii, and thus, the λ value remains constant throughout the series. Thus, this system can be considered to form a true homogeneous series. The experimentally observed k_q values are well below the diffusion-controlled rate constants, and thus, the saturation of rate constants at the diffusion level is not observed as expected from Rehm–Weller model. Furthermore, triplet-state energy of phenol has been estimated to be 3.5 eV, and thus, the formation of the triplet-state phenoxyl radical as product is unlikely.²¹ From these arguments we conclude that if a suitable homogeneous reaction series is chosen with appreciable change in ΔG° , but maintaining other parameters such as λ and d constant, it is possible to observe the Marcus inverted region in the bimolecular charge-separation reactions. Thus, we can categorically state that in the photoinduced electron-transfer reactions of $\text{Ru}(\text{NN})_3^{2+}$ with phenolate ions all the predictions of the Marcus theory on the kinetics of ET have been fully verified.³⁸

References and Notes

- (1) Chanon, M.; Fox, M. A. *Photoinduced Electron Transfer*; Elsevier: New York, 1988; Vol. 1–4.
- (2) Kavarnos, G. J. *Fundamentals of Photoinduced Electron Transfer*; VCH: New York, 1993.
- (3) Bolton, J. R.; Mataga, N.; McLendon, G., Eds. *Electron Transfer in Inorganic, Organic and Biological Systems*; Advances in Chemistry Series 228; American Chemical Society: Washington, DC, 1991.
- (4) Mattay, J., Ed. *Photoinduced Electron Transfer*; Topics in Current Chemistry 163; Springer-Verlag: Berlin, 1992.
- (5) Marcus, R. A.; Sutin, N. *Biochim. Biophys. Acta* **1985**, *811*, 265.
- (6) Ebersson, L. *Electron-Transfer Reactions in Organic Chemistry*; Springer-Verlag: Berlin, 1987.
- (7) Astruc, D. *Electron Transfer and Radical Processes in Transition Metal Chemistry*; VCH: New York, 1995.
- (8) Suppan, P. *Top. Curr. Chem.* **1992**, *163*, 95.
- (9) Miller, J. R.; Calcaterra, L. T.; Closs, G. L. *J. Am. Chem. Soc.* **1984**, *106*, 3047. Closs, G. L.; Miller, J. R. *Science* **1988**, *240*, 440. Liang, N.; Miller, J. R.; Closs, G. L. *J. Am. Chem. Soc.* **1990**, *112*, 5353.
- (10) Gould, I. R.; Ege, D.; Moser, J. E.; Farid, S. *J. Am. Chem. Soc.* **1990**, *112*, 4290. Gould, I. R.; Farid, S. *J. Phys. Chem.* **1992**, *96*, 7635. Arnold, B. R.; Noukakis, D.; Farid, S.; Goodman, J. L.; Gould, I. R. *J. Am. Chem. Soc.* **1995**, *117*, 4399. Gould, I. R.; Farid, S. *Acc. Chem. Res.* **1996**, *29*, 522.
- (11) McCleskey, T. M.; Winkler, J. R.; Gray, H. B. *J. Am. Chem. Soc.* **1992**, *114*, 6935. McCleskey, T. M.; Winkler, J. R.; Gray, H. B. *Inorg. Chim. Acta* **1994**, *225*, 319.
- (12) Gramp, G. *Angew. Chem., Int. Ed. Engl.* **1993**, *32*, 691. Kikuchi, K.; Miwa, T.; Takahashi, Y.; Ikeda, H.; Miyashi, T. *J. Phys. Chem.* **1993**, *97*, 5070.
- (13) Murtaza, Z.; Graff, D. K.; Zipp, A. P.; Worl, L. A.; Jones, W. F., Jr.; Bates, W. D.; Meyer, T. J. *J. Phys. Chem.* **1994**, *98*, 10504.
- (14) Turro, C.; Zaleski, J. M.; Karabatsos, Y. M.; Nocera, D. G. *J. Am. Chem. Soc.* **1996**, *118*, 6060 and references therein.
- (15) Hug, G. L.; Marciniak, B. *J. Phys. Chem.* **1995**, *99*, 1478.
- (16) Juris, A.; Balzani, V.; Barigelli, F.; Campagna, S.; Belser, P.; Von Zelewsky, A. *Coord. Chem. Rev.* **1988**, *84*, 85. Krause, R. A. *Struct. Bonding* **1987**, *67*, 1.
- (17) Kalyanasundaram, K. *Coord. Chem. Rev.* **1982**, *46*, 159. Kalyanasundaram, K. *Photochemistry of Polypyridine and Porphyrin Complexes*; Academic Press: New York, 1992.
- (18) Kalyanasundaram, K.; Gratzel, M., Eds. *Photosensitization and Photocatalysis Using Inorganic and Organometallic Compounds*; Kluwer Academic: Dordrecht, 1993.
- (19) Connolly, J. S., Eds. *Photochemical Conversion and Storage of Solar Energy*; Academic Press: New York, 1981.
- (20) Gratzel, M., Eds. *Energy Resources through Photochemistry and Catalysis*; Academic Press: New York, 1983.
- (21) Miedlar, K.; Das, P. K. *J. Am. Chem. Soc.* **1982**, *104*, 7462.
- (22) Rajagopal, S.; Allen Gnanaraj, G.; Mathew, A.; Srinivasan, C. *J. Photochem. Photobiol. A* **1992**, *69*, 83.
- (23) Vera, D. M.; Arguello, G. A.; Arguello, G. A.; Gsponer, H. E. *J. Photochem. Photobiol. A* **1993**, *76*, 13. Senz, A.; Gsponer, H. E. *J. Colloid Interface Sci.* **1994**, *165*, 60 and references therein.
- (24) Rillema, D. P.; Jones, D. S.; Woods, C.; Levy, H. A. *Inorg. Chem.* **1992**, *31*, 2935.
- (25) Kawanishi, Y.; Kitamura, N.; Tazuke, S. *Inorg. Chem.* **1989**, *28*, 2968. Haga, M. A.; Dodsworth, E. S.; Eryavec, G.; Seymour, P.; Lever, A. B. P. *Inorg. Chem.* **1985**, *24*, 1901. Liu, C. T.; Bottcher, W.; Chou, M.; Cruz, C.; Sutin, N. *J. Am. Chem. Soc.* **1976**, *98*, 6536. Brewer, K. J.; Murphy, W. R., Jr.; Spurlin, S. R.; Peterson, J. D. *Inorg. Chem.* **1986**, *25*, 882. Kitamura, N.; Rajagopal, S.; Tazuke, S. *J. Phys. Chem.* **1987**, *91*, 3767.
- (26) Ramamurthy, P. *Chem. Educ.* **1993**, *9*, 56.
- (27) Parsons, B. J.; Beaumont, P. C.; Navaratnam, S.; Harrison, W. D.; Akasheh, T. S.; Othman, M. *Inorg. Chem.* **1994**, *33*, 157. Akasheh, T. S.; Beaumont, P. C.; Parsons, B. J.; Phillips, G. O. *J. Phys. Chem.* **1986**, *90*, 5651. Neshvad, G.; Hoffman, M. Z. *J. Phys. Chem.* **1989**, *93*, 2445.
- (28) Debye, P. *Trans. Electrochem. Soc.* **1942**, *82*, 265. Brede, O.; Orthner, H.; Zubarev, V.; Hermann, R. *J. Phys. Chem.* **1996**, *100*, 7097.
- (29) Maruyama, Y.; Kaizu, Y. *J. Phys. Chem.* **1995**, *99*, 6152.
- (30) Jakobsen, S.; Mikkelsen, K. V.; Pedersen, S. U. *J. Phys. Chem.* **1996**, *100*, 7411.
- (31) Armstrong, D. A.; Sun, Q.; Schuler, R. H. *J. Phys. Chem.* **1996**, *100*, 9892.
- (32) Arnett, E. M.; Amarnath, K.; Harvey, N. G.; Venimadhavan, S. *J. Am. Chem. Soc.* **1990**, *112*, 7346.
- (33) Bordwell, F. G.; Cheng, J. P. *J. Am. Chem. Soc.* **1991**, *113*, 1736.
- (34) Andrieux, C. P.; Saveant, J. M. In *Investigation of Rates and Mechanisms of Reactions*; Bernasconi, C. F., Ed.; John Wiley: New York, 1986; Vol. 6, Chapter 7. Denisov, E. T.; Khudyakov, I. V. *Chem. Rev.* **1987**, *87*, 1313. Hapiot, P.; Pinson, J.; Yousfi, N. *New J. Chem.* **1992**, *16*, 877.
- (35) Gould, I. R.; Noukakis, D.; Gomez-Jahn, L.; Goodman, J. L.; Farid, S. *J. Am. Chem. Soc.* **1993**, *115*, 4405.
- (36) Doolen, R.; Simon, J. D.; Baldrige, K. K. *J. Phys. Chem.* **1995**, *99*, 13938.
- (37) Clark, C. D.; Hoffman, M. Z. *J. Phys. Chem.* **1996**, *100*, 14688.
- (38) Marcus, R. A. *Angew. Chem., Int. Ed. Engl.* **1993**, *32*, 1111.